RESEARCH ARTICLE

THE EFFECTS of DIFFERENT HEAT TREATMENT and COATING TECHNIQUES on X120CrMo29-2 MARTENSITIC STAINLESS STEEL

Esad KAYA[1*], Mustafa ULUTAN[2], Ahmet AKBULUT[3]

[*1]Eskişehir Osmangazi University, Faculty of Engineering and Architecture, Division of Mechanical Engineering, esatkaya@ogu.edu.tr, ORCID: 0000-0002-7332-6154
[2]Eskişehir Osmangazi University, Faculty of Engineering and Architecture, Division of Mechanical Engineering, mulutan@ogu.edu.tr, ORCID: 0000-0003-1821-6486
[3]IGSAS, Kütahya Integrated Facilities, Research and Development Center Department, ahmet.akbulut@igsas.com.tr, ORCID: 0000-0001-7522-5341

ABSTRACT

This research article investigated the effects of various heat treatment and coating processes on the tribological performance of X120CrMo29-2 martensitic stainless steel materials. The effects of deep cryogenic treatment, plasma nitriding, and high-velocity oxy-fuel (HVOF) thermal spraying methods on microstructural, mechanical, and tribological properties were investigated. The as-quenched condition was taken as the reference group. In the experimental studies, it was observed that the wear resistance of the deep cryogenic heat treated and coated samples were improved 1,2-6,7 times in comparison to the reference group. In terms of microstructure and mechanical properties, more homogeneous general structural hardness was obtained in the deep cryogenically treated samples, while high surface hardness values (980 $HV100_{gf,10\ sec}$) were found in coated samples. In terms of tribological properties, it was observed that the wear resistance of the coated samples was higher than the deep cryogenically treated samples. It is seen that nitride coatings have superior tribological properties to the HVOF sprayed sample. The lowest coefficient of friction (COF) and highest wear resistance was observed in plasma nitrided samples.

Keywords: *Wear, Friction, Tribology, Coatings, Nitriding*

1. INTRODUCTION

Martensitic stainless steels have superior mechanical properties to other stainless steel groups due to the high Cr and C ratio in their content. [1]. For this reason, martensitic stainless steels are used in different areas such as turbine blades, bearings, surgical apparatus, and machine parts that provide fluid transport in corrosive environments [2, 3]. Although martensitic stainless steels exhibit high mechanical and tribological properties, this is insufficient for some industrial application areas. Therefore, martensitic stainless steels properties still need to be improved for some applications. This situation is primarily encountered in pump impellers, balancing discs, rotors, and valves used to transport hot corrosive fluids where high thermal stability is required. [1]. Different surface engineering techniques can be applied to improve the surface properties of martensitic stainless steels

and create new areas of use [4-6]. One of these techniques is the deep cryogenic heat treatment process which is additive process to quenching. Deep cryogenic heat treatment is complementary to the traditional heat treatment procedure. [7]. In this process, the austenite, which remains retained in the microstructure after quenching, is transformed into martensite and forms secondary carbide with the free carbon element. [8]. These transformations increase the overall hardness and wear resistance of the material. In addition, different coating methods are used to improve the surface properties of martensitic stainless steels. One of these is the high-velocity oxy-fuel (HVOF) technique. In this process, the powder mixture brought to a spray gun chamber with carrier gas is burned with a liquid-gas fuel mixture and transferred to the surface to be coated in semi-melt form. With this process, coatings with a thickness of ~200 μm with low porosity on the surface can be obtained [9, 10]. The HVOF technique can be applied to any machine part subject to different types of wear under impact load [11]. The resulting coatings have relatively low porosity, high deposition volume, and hardness [12]. In line with these desired properties and due to the high melting temperature, carbides and oxides (WC, TiC, Al_2O_3, etc.) are highly preferred in this method [13]. Another method used to improve the surface properties of stainless steel is the nitriding method. Today, nitriding can be applied with gas, salt bath, plasma ion nitriding types [14]. Ammonia and cyanide salts are used as N_2 donor media in gas and salt bath methods. Machine parts made of steel materials pose major disadvantages if the processing temperatures exceed 700°C for effective coating thickness and low processing time [1]. For this reason, the plasma nitriding process, which is carried out in the ionized gas phase and at low temperature, is highly preferred [15]. This process is a plasma assisted thermochemical process and uses the workpiece as a cathode. As a result of ionized gas bombardment, coating layers with high load carrying ability and hardness are obtained on the surface [16]. These structures formed on stainless steel surfaces are supersaturated γ-N and S phases in terms of N_2 [1, 17]. In the studies, it is seen that the plasma-assisted ion nitriding process at low temperatures prevents the formation of hard and brittle (Metal)$_2$N. It is known that nitrides formed from this chemical composition deteriorate the tribomechanical properties of the γ-N and S phases [1, 16, 17]. Therefore, when low temperature plasma assisted nitriding, carburizing, nitrocarburizing processes are investigated, it is known that these processes improve the mechanical, microstructural and tribological properties of different types of stainless steels and non-ferrous materials [14, 18, 19].

When the studies in the literature are examined, it is pretty common to improve the surface properties of austenitic stainless steels due to high corrosion, low hardenability, and wear resistance [20-22]. It has been observed that studies on the improvement of the properties of martensitic stainless steels are few. In this study, the tribomechanical properties of X120CrMo29-2 quality martensitic stainless steel, which is frequently used to manufacture pump impeller material carrying corrosive fluid at high temperatures, were tried to be improved by different heat treatment and coating methods.

2. MATERIAL and METHOD

2.1.Material

Commercial type X120CrMo29-2 martensitic stainless steel material obtained from IGSAŞ (Istanbul Gübre Sanayi Anonim Şirketi) was used in the study. The material was formed into cubes with a side of 12.70 mm by the EDM method. Conventional metallographic sample preparation processes were applied to all cube samples' surfaces and polished so that their average surface roughness was below 0.5 μm. Table 1 shows the chemical composition of the material and the control groups in the

experimental studies. Experimental studies were carried out in five different control groups. The first group samples were taken as a reference (Q) and, after austenitization at 840°C for 1 hour, quenched and tempered at 200°C for 3 hours. In the second group of samples (QC), deep cryogenic treatment was applied in addition to the traditional heat treatment procedure. The process was carried out in an MMD Cryo brand computer-controlled device. The specimen was kept at a deep cryogenic temperature of -196°C at a 2°C/min rate for 36 hours. After processing, the sample was tempered at 200°C for 1 hour. Plasma nitriding was applied to the third and fourth group samples (N1, N2). After polishing the sample surfaces, metallographic processes were subjected to plasma nitriding at 450°C and 520°C temperatures, during a 12-hour waiting period under 2 mbar pressure in 75% N2 + 25% H2 gas atmosphere. After the process, the samples were left to cool to room temperature in a vacuum media. WC-Co coatings were applied to another group of samples by the high-velocity oxy-fuel method (HVOF). The process was carried out on a Metco Diamond Jet 2700 device. Mixture powders consisting of 83% WC and 17% Co by mass. During the process, powders were heated to 165 °C and the workpiece temperature to 204 °C. The process was operated at a pressure of 0.6 MPa using air as the carrier gas. The powder feed rate was used as 30 gr/min.

2.2. Method

Of the samples whose production processes were completed, coated samples were cut with the wet abrasive cutting method, and their surfaces were polished. Metallographic polishing was applied to one surface of the heat-treated samples. After polishing, the surfaces were etched with 2% Nital solution. The microstructures of the etched samples were investigated by SEM-EDS analysis. JEOL JSM-5600LV scanning electron microscope was used for analysis. EDS analyzes were also performed at the time of SEM acquisition. X-ray diffraction technique was used to determine the phases formed in the samples. Panalytical Empyrean device was used in the experiments. The XRD examination was performed with the Cu-K$_\alpha$ radiation and a wavelength of 1.54060 Å. For coatings and samples, X-ray diffraction patterns were obtained by scanning at 2θ angles between 20°-100° with a step size of 0.02 at a speed of 0.5°/min. The obtained diffraction patterns were analyzed with the X'pert HighScore Plus package program. The hardness values of the samples were made using the microhardness measurement technique. Hardness measurements were made on a Future Tech FM-800 type device. The hardness of the samples, which were subjected to heat treatment and plasma nitriding, was determined at 25 gf load and 10 seconds dwelling time, and the hardness of the HVOF sample was determined at 100 gf load and 10 seconds dwelling time. The wear tests were performed on all specimens in spherical-disc type geometry in a CSM Tribometer device per ASTM G-99 standards. In the experiments, balls with Ø 3 mm diameter, 91.6 HRA hardness, 700 GPa elastic modulus, certified spherical, with 96% WC-4% Co content, were used as counter body material. The experiments were carried out with a load of 5 N, a diameter of 3 mm, a wear distance of 50 meters, and a sliding speed of 3 cm/s (189 rpm). The formed worn channels on the surfaces were measured with Mitutoyo SJ-400 surface roughness device and Gauss filtering technique in ISO R97 standard. Worn channels were observed by SEM-EDS techniques to examine the wear mechanisms in detail.

Table 1. Chemical composition of martensitic stainless steel material used in experimental studies and control groups.

The Chemical Content of X120CrMo29-2

C	Si	Cr	Mn	Mo	Fe

1,10	2,00	28,00	1,00	2,25	Bal.
Control Groups					
Specimen	**Description**				
Q	1 hour austenitizing at 810°C +Quenching 3 hours at 300°C Tempering				
QC	Q+36 hours 196°C Deep Cryogenic Treatment + 1-hour Tempering at 200°C				
N1	Q+ 450°C Nitriding Process				
N2	Q+ 420°C Nitriding Process				
HVOF	Q+ HVOF WC-Co Coating				

3. RESULTS AND DISCUSSION

3.1. Microstructure Analysis

Figure 1 shows SEM-EDS analyzes of martensitic stainless steel samples with different heat treatments and coatings. When the samples are examined in general, there are no discontinuities and defects in the structures due to production, heat treatment, and coating processes. Figures 1.a-b show the neat quenching (Q) and deep cryogenically treated (QC) samples, respectively. One can be understand from the figure, the microstructure is composed of perlite and cementite phase due to the high temperature tempering process. In the deep cryogenic treated sample, it is seen that the structure is preserved in a similar situation. It has been observed that the general improvement mechanisms seen in the microstructure of tool steels by deep cryogenic treatment are not very effective in martensitic stainless steels [23].
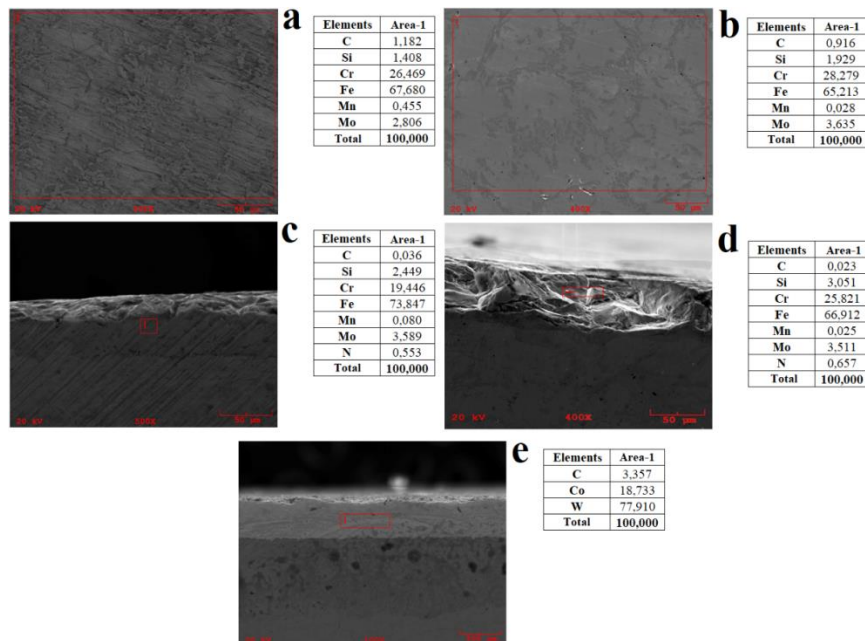
Figure 1. SEM-EDS analyzes of samples: a)Q, b)QC, c)N1, d)N2, e)HVOF.

Figure 1.c-d shows cross-sectional SEM-EDS analyzes of plasma nitrided samples. It is seen that there is a nitriding layer with a homogeneous thickness distribution of 50-70 μm. In addition, the nitriding layer formed does not contain any defects and voids. This situation is an indication that the nitriding layer production parameters were selected effectively. When the EDS analyzes are examined, it is seen that the obtained layer mainly contains Fe-Cr-N. The substrate's high Fe and Cr content indicates that the resulting nitriding layer is predominantly composed of Fe-Cr-N compounds. Figure 1.d shows the cross-sectional SEM-EDS analysis of the WC-Co coated sample with the HVOF technique. When the coating cross-section SEM photograph is examined, it is seen that the coating forms homogeneously on the surface without any porosity, cracks, or discontinuities along the surface. It is seen that the obtained coating layer thickness is approximately 200 μm. Figure 2 shows the X-ray diffraction patterns of the samples. When the diffraction pattern of the conventional heat-treated and deep cryogenic treated samples (Figure 2.a-b) is examined, it is seen that the structures are composed of carbide, martensite, and austenite phases. It is observed that the intensity of the carbide peaks increased and the intensity of the austenite peaks decreased in the deep cryogenically treated sample. It is thought that after the applied deep cryogenic heat treatment, the retained austenite in the microstructure turns into martensite and forms a carbide with the free element Cr. When the plasma nitrided samples are examined (Figure 2.c-d), it is seen that the structures are composed of nitrides containing Fe and Cr. In addition, it was determined that $(Metal)_2N$ was not observed, which is extremely brittle and hard. This observation shows that the applied process is carried out under the most suitable conditions. Figure 2.d shows the diffraction pattern of the WC-Co coated sample with the HVOF technique. When the obtained diffraction pattern is examined, it is seen that the structure mainly consists of WC peaks and rarely Co peaks. 83% by mass of the powder mixture desired to be coated on the surface contains WC. For this reason, it is seen that the peak intensities obtained are compatible with the mass content thrown to the surface.
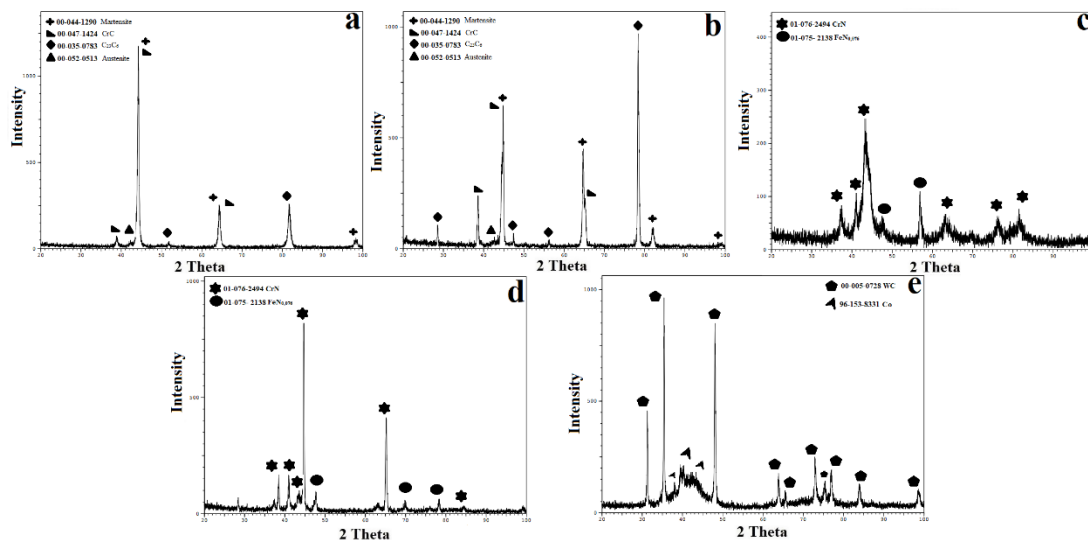
Figure 2. X-ray diffraction patterns of the samples: a)Q, b)QC, c)N1, d)N2, e)HVOF.

3.2. Mechanical and Tribological Analysis

Figure 3. It shows the hardness values of the samples. While the hardness values of the conventional heat-treated and deep cryogenic heat-treated samples are average (480 $HV_{25gf,10s}$), the hardness values of the plasma nitrided and HVOF-coated samples show the change of the coating surface towards the substrate material. Since WC is one of the hardest carbides known, the highest average hardness values are seen in the sample coated with WC-Co with the HVOF technique (980 $HV_{100gf,10s}$). When the hardness values obtained were compared with the SEM analysis of the coating (Figure 1-e), it was observed that high hardness behavior was exhibited throughout the coating section and decreased by 50% in the transition region. Another high hardness value is seen in plasma nitrided samples. The hardness measurements show that the hardness varies between 700 HV and 900 HV throughout the layer thickness. The average hardness values obtained from the nitriding process at 450°C and 520°C were measured as 715 $HV_{25gf,10s}$ and 665 $HV_{25gf,10s}$, respectively. It is seen that the obtained hardness values are consistent with the cross-sectional SEM analyzes of the nitride layers. It is thought that the high hardness obtained by nitriding at low temperatures is due to the CrN layers formed with low thermal stress. Healing effects such as austenite-martensite transformation and secondary carbide formation provided by the deep cryogenic heat treatment in the microstructure are also seen in the hardness values. With the measurements made, it is seen that the average hardness value of the deep cryogenic treated sample increased by about 10% compared to the reference sample (494 $HV_{25gf,10s}$).
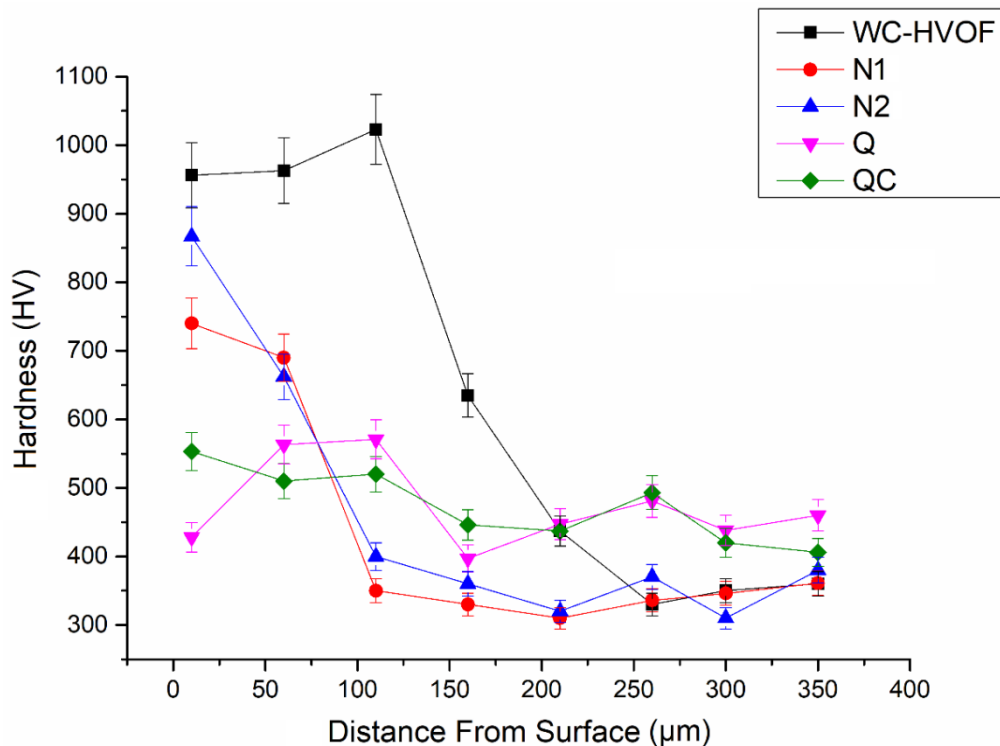
Figure 3. Hardness variation graphs of the samples.

Figure 4. shows the specific wear rate-friction coefficient variation graph of all samples. It is seen that there is a parallelism between the change in friction coefficient values and the change in wear rates. As expected, wear, and friction behavior improvements were observed in all applied heat treatments and coating techniques compared to the reference group. As can be seen from the figure, the highest wear rate of $8.77 \times 10^{-5} mm^3/Nmm$ was determined in the reference sample. The application of deep cryogenic treatment increased the wear resistance by about 10%. With the WC-Co coating applied with the HVOF technique, the wear resistance was improved by 20% compared to the reference sample. On the other hand, the plasma nitriding process improved the wear resistance of the samples between 5.0 and 6.7 times.
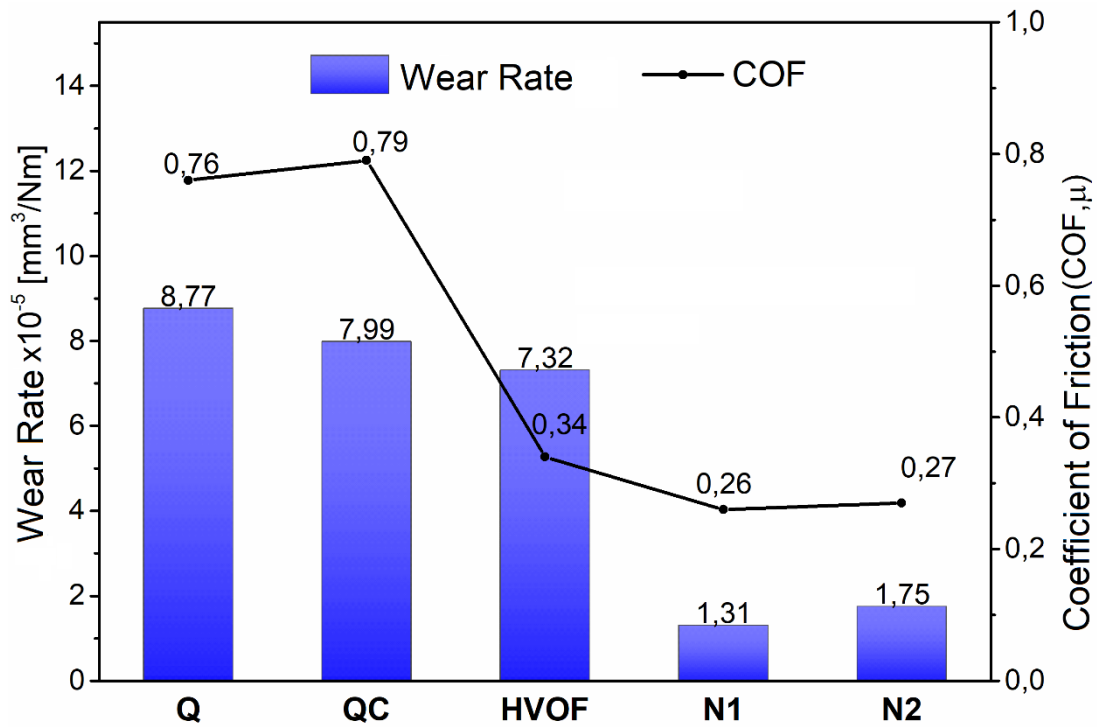
Figure 4. The wear rate of the samples and the average friction coefficient variation graph.

Figure 5. shows the instantaneous COF change graph of all samples during the wear test. As a result of the experiments, the lowest average friction coefficient is observed in plasma nitrided samples (~0.25). The highest average friction coefficient was observed in the heat-treated groups as expected (~0.75). The friction coefficient data obtained from the experiment are similar to the wear rates. When the friction behaviors are examined, it is seen that the friction behavior of the plasma nitrided samples is in a regular regime at low values. The main reason for the regular regime in nitrided layers is that the abrasive three bodies are not formed during wear, and the wear behavior is not exacerbated. The high surface roughness of the HVOF coating layer compared to plasma nitrided coatings causes hard WC hard particles to break off from the surface during the wear test. They are included in the contact

area of the broken particles again and react with O_2 and N_2 to form tribochemical residues. These formed structures trigger three-body abrasive wear, causing an increase in the wear rate relatively compared to nitride layers. Extreme fluctuations were observed in the reference and deep cryogenic treated samples, where the highest COF values were observed. The main reason for this situation is the direct interaction of the opposite body at the contact point, which shows that three-body abrasive wear is effective.
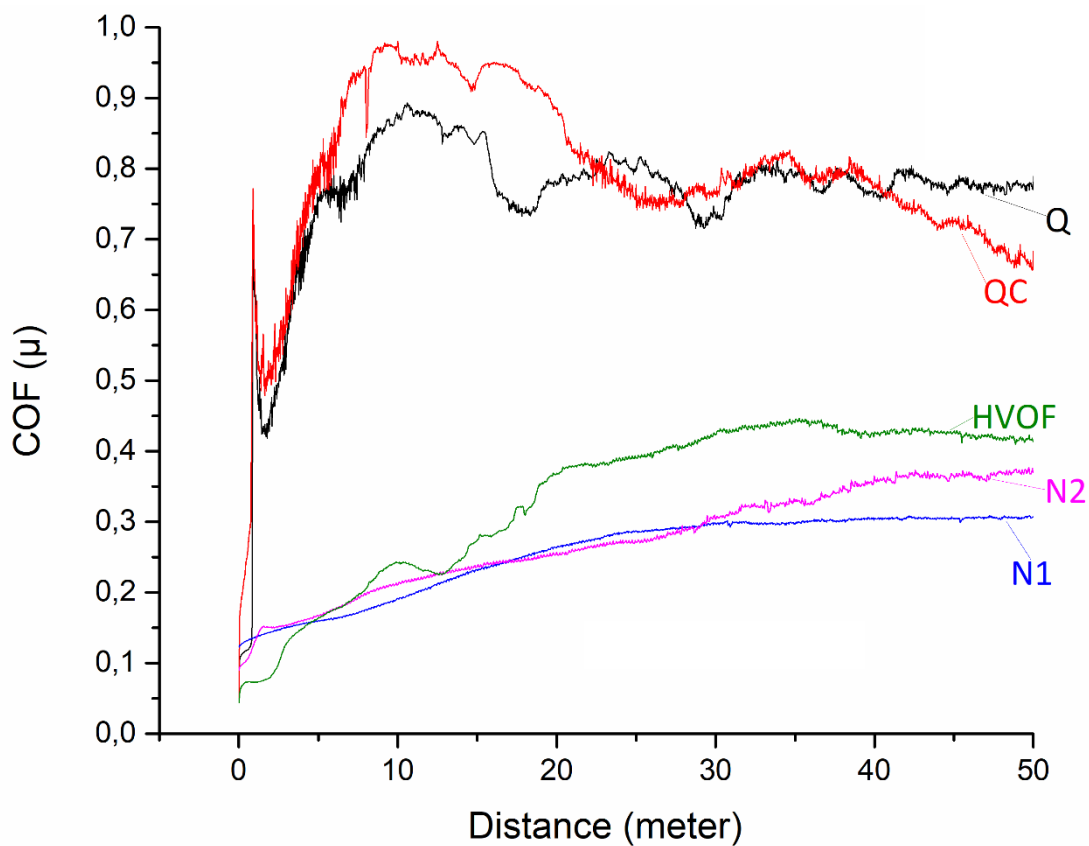
Figure 5. Instantaneous COF alteration graph of the samples during the wear test.

Figure 6 shows the SEM-EDS analyses of the samples after the wear test. When the surface analysis of the quenched and deep cryogenically treated samples, which have the lowest wear resistance, is examined, deep abrasive traces (Figure 6.b-5) and oxidation traces (Figure 6.a-1) are observed. It is thought that an active three-body abrasive wear mechanism forms these deep scars. When the EDS analysis of the surfaces was examined, it was determined that the highest amount of W, Co, and O. Therefore, it is seen that the dominant wear mechanisms are adhesive and abrasive. When the wear surface SEM-EDS analyses of nitride coatings are examined exhibiting low friction behavior (Figure 6.c-d), it is seen that the effects of abrasive and adhesive wear are pretty superficial and low as expected. It is seen that the worn nitriding layers have the lowest ratio of W, Co, and O. It has been

observed that these layers with high stability did not initiate three-body abrasive wear during wear and prevented the aggravation of wear. When the HVOF coating sample was examined, it was determined that the abrasive traces formed on the surfaces were shallow according to the quenching and deep cryogenic treatment conditions but deep compared to the nitriding layers. Despite their high hardness properties, the high average surface roughness of the HVOF layers reduces the load-bearing ability of these layers. The parts that break off from the surface with increasing wear distance (Figure 6.e-3) intensify the wear and decrease the wear resistance. For this reason, with increasing wear distance, they wear more than nitride layers with thinner thickness and become insufficient.
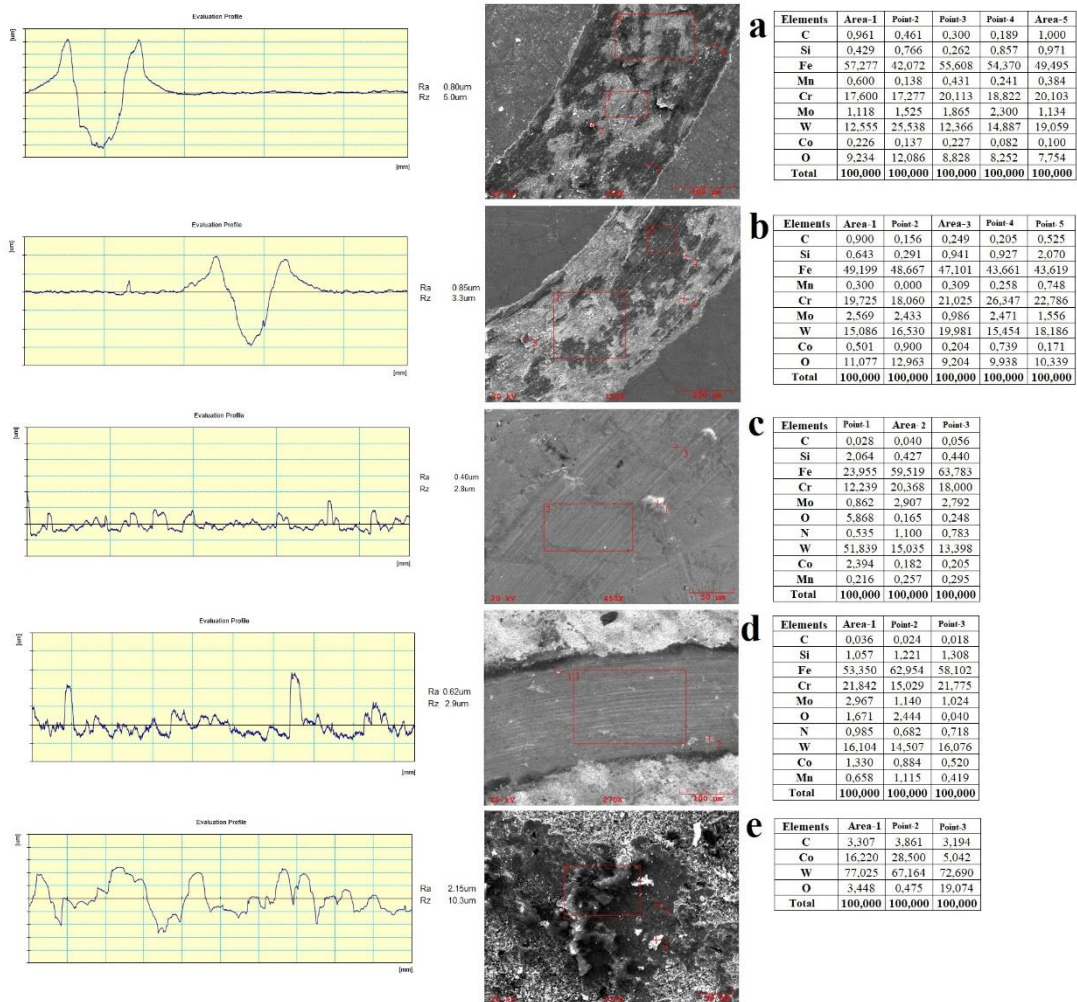
Figure 6. Wear SEM-EDS analysis of samples: a)Q, b)QC, c)N1, d)N2, e)HVOF.

6. CONCLUSION

This study applied different heat treatments and coating techniques on X120CrMo29-2 martensitic stainless steels. By examining the microstructure and mechanical properties of the samples, the most suitable surface modification process was tried to be determined. The findings obtained in the experimental studies are summarized as follows:

Heat treatments and coatings were successfully applied in all control groups. It has been determined that there are no cracks, gaps, or discontinuities in the heat treatment applications and on the coating surfaces.

In the X-ray diffraction analysis, decreases in the austenite phase peak intensities were detected in the deep cryogenically treated samples. It was determined that the nitride layers were mainly composed of Cr and Fe. It was determined that WC peaks were dominant in the HVOF layer.

Compared to the reference sample (480 $HV_{25gf,10s}$), a 10% increase in hardness was detected in deep cryogenically treated samples and 2 to 3 times in plasma nitride and HVOF coatings. The highest in-depth hardness increase was obtained with HVOF coatings (980 $HV_{100gf,10s}$).

The lowest average COF was observed in the plasma nitrided layers (~0.25), while the highest average COF was found in the reference group (~0.75).

In all applied heat treatments and coating techniques, the wear resistance has been increased compared to the reference sample. While the highest wear rate was observed in the reference sample with $8.77 \times 10^{-5} mm^3/Nmm$, the lowest was found in the plasma nitrided sample at 450°C with $1.31 \times 10^{-5} mm^3/Nmm$.

ACKNOWLEDGMENT

REFERENCES

[1] Lee, I., (2019), Combination of plasma nitriding and nitrocarburizing treatments of AISI 630 martensitic precipitation hardening stainless steel. Surface and Coatings Technology, 376: p. 8-14.

[2] Lyu, Z., Yutaka, S., Shun, T., Yue, Z., Jinlong, J., Aiping, W., (2021), Microstructural distribution and anisotropic tensile behavior in a 2Cr13 martensitic stainless steel thin wall fabricated by wire arc additive manufacturing. Materials Today Communications, 29.

[3] Baghjari, S.H., Akbari, S., (2013), Effects of pulsed Nd:YAG laser welding parameters and subsequent post-weld heat treatment on microstructure and hardness of AISI 420 stainless steel. Materials & Design, 43: p. 1-9.

[4] Alonso, F., Arizaga, A., Garcia, J., Oñate, I., (1994),Tribological effects of yttrium and nitrogen ion implantation on a precipitation hardening stainless steel. Surface and Coatings Technology, 66(1-3): p. 291-295.

[5] Tesi, B., Bacci, T., Poli, G., (1985), analysis of surface structures and of size and shape variations in ionitrided precipitation hardening stainless steel samples. Vacuum, 35(8): p. 307-314.

[6] Leyland, A., Lewis, D., Stevensom, P., Matthews, A., (1993), Low temperature plasma diffusion treatment of stainless steels for improved wear resistance. Surface and Coatings Technology, 62(1-3): p. 608-617.

[7] Sert, A., (2020), AISI M2 Takım Çeliğinin Mikroyapısı ve Mekanik Davranışları Üzerine Derin Kriyojenik Isıl İşlemin ve Temperlemenin Etkisi. Deu Muhendislik Fakultesi Fen ve Muhendislik Dergisi, 22(66): p. 801-811.

[8] Kara, F., Özbek, O., Özbek, N., Uygur, İ., (2021), Investigation of the Effect of Deep Cryogenic Process on Residual Stress and Residual Austenite. Gazi Journal of Engineering Sciences, 7(2): p. 143-151.

[9] Mann, B., Arya, V., (2003), HVOF coating and surface treatment for enhancing droplet erosion resistance of steam turbine blades. Wear, 254(7-8): p. 652-667.

[10] Mann, S., Arya, V., Joshi, P., (2005), Advanced High-Velocity Oxygen-Fuel Coating and Candidate Materials for Protecting LP Steam Turbine Blades Against Droplet Erosion. Journal of Materials Engineering and Performance, 14(4): p. 487-494.

[11] Moskowitz, L., Trelewicz, K., (1997), HVOF coatings for heavy-wear, high-impact applications. Journal of Thermal Spray Technology, 6(3): p. 294-299.

[12] Buytoz, S., Ulutan, M., Islak, S., Kurt B., Çelik, O.N., (2013), Microstructural and Wear Characteristics of High Velocity Oxygen Fuel (HVOF) Sprayed NiCrBSi–SiC Composite Coating on SAE 1030 Steel. Arabian Journal for Science and Engineering, 38(6): p. 1481-1491.

[13] Ozkavak, H.V., Sahin, S., Sarac, M.F., Alkan, Z., (2020), Wear properties of WC–Co and WC–CoCr coatings applied by HVOF technique on different steel substrates. Materials Testing, 62(12): p. 1235-1242.

[14] Cheng, Z., Li, C., Dong, H., Bell, T., (2005), Low temperature plasma nitrocarburising of AISI 316 austenitic stainless steel. Surface and Coatings Technology, 191(2-3): p. 195-200.

[15] Reddy, C.A.K., Srinivasan, T., Venkatesh, B., (2021), Srinivasan, and B. Venkatesh, Effect of plasma nitriding on M50 NiL steel – A review. Materials Today: Proceedings.

[16] Zhang, Z.L., Bell, T., (2013), Structure and Corrosion Resistance of Plasma Nitrided Stainless Steel. Surface Engineering, 1(2): p. 131-136.

[17] Menthe, E., Rie, K.T., Schultze, S.C., Simson, S., (1995), structure and properties of plasma-nitrided stainless steel. Surface and Coatings Technology, 74-75: p. 412-416.

[18] Bell, T., Sun, Y., Suhadi, A., (2000), Environmental and technical aspects of plasma nitrocarburising. Vacuum, 59(1): p. 14-23.

[19] Lei, M.K., Ou, Y.X., Wang, K.S., Chen, L., (2011), Wear and corrosion properties of plasma-based low-energy nitrogen ion implanted titanium. Surface and Coatings Technology, 205(19): p. 4602-4607.

[20] Haruman, E., Sun, Y., Adenan, M.S., (2020), A comparative study of the tribocorrosion behaviour of low temperature nitrided austenitic and duplex stainless steels in NaCl solution. Tribology International, 151.

[21] Yangyang, L., Dong, L., Heng, M., Xiliang, L., Meihong, W., Jing, H., (2021), Enhanced plasma nitriding efficiency and properties by severe plastic deformation pretreatment for 316L austenitic stainless steel. Journal of Materials Research and Technology, 15: p. 1742-1746.

[22] Naofumi, O., Koyo, M., Mitsuhiro, H., Kenji, K., (2021), Investigation of admixed gas effect on plasma nitriding of AISI316L austenitic stainless steel. Vacuum, 193.

[23] Hariharan, K.B., Savaranan, S., Parkunam, N., (2020), Life time improvement of D7 tool steel by cryogenic treatment. Materials Today: Proceedings, 21, p. 619-621.